Effects of the electron-phonon coupling activation in collision cascades.

Eva Zarkadoula,[1] German Samolyuk,[1] and William J. Weber[2,1]

[1] *Materials Science & Technology Division, Oak Ridge National Laboratory, Oak Ridge, TN 37831, USA*
[2] *Department of Materials Science & Engineering, University of Tennessee, Knoxville, TN 37996, USA*

Using the two-temperature (2T-MD) model in molecular dynamics simulations, we investigate the condition of switching the electronic stopping term off when the electron-phonon coupling is activated in the damage production due to 50 keV Ni ion cascades in Ni and equiatomic NiFe. Additionally we investigate the effect of the electron-phonon coupling activation time in the damage production. We find that the switching condition has negligible effect in the produced damage, while the choice of the activation time of the electron-phonon coupling can affect the amount of surviving damage.

Keywords: Molecular dynamics, Two-temperature model, Electronic effects, Nickel and nickel alloys, Cascades

Molecular dynamics (MD) simulations is a technique that has been widely used to investigate ion irradiation effects in matter [1, 2]. Using the equation of motion to calculate the atom trajectories and describe the system status at any point during the simulation, MD simulations are an important tool to gain insights at the atomic level, and provide information on the processes that take place in very small length-scales, in the range of a few angstroms, within time of some tens of picoseconds. For energy events of up to a few keV, this classical approach for ballistic collision processes is accurate, and has revealed important information on primary radiation damage processes and cluster formation [3–9]. For irradiation with ions of higher energy (from a few tens of keV), the two-temperature (2T-MD) model [10, 11] in MD simulations is a more realistic approach, as it takes into account the energy exchange between the atomic and the electronic subsystems [12, 13]. In the 2T-MD model, the excited electrons can act as a heat sink or a heat bath [10, 14], which can affect damage production, defect recovery and cluster formation.

Recent simulations of 30 and 50 keV Ni cascades in Ni and Ni-based solid solution alloys [15, 16] have shown that, compared to classical MD cascades and cascades where only the electronic stopping are taken into account, the 2T-MD model, which includes the electron-phonon (e-ph) coupling in addition to the electronic stopping, results in a smaller amount of damage and more isolated vacancies and interstitials. In the present paper, we investigate the effect of deactivating the electronic stopping mechanism when the e-ph coupling is turned-on, as well as the effect of the e-ph coupling activation time in the damage production.

For our simulations we use the MD package DL_POLY [17], where the 2T-MD model [10, 11] algorithms are incorporated. In the 2T-MD model, as described by Duffy and Rutherford [10, 11], the equation of motion used in classical MD simulations is modified (Eq.1), and contains a friction term γ_i to include the energy loss to electrons, and a term (stochastic force $\mathbf{F}_i(t)$) to include the energy gain due to interactions with the electrons of the system. The friction term γ_i consists of a term γ_s for the electronic stopping, and a term γ_p to account for the e-ph coupling, which is activated at time t_{eph}.

$$m_i \frac{\partial \mathbf{v}_i}{\partial t} = \mathbf{F}_i(t) - \gamma_i \mathbf{v}_i + \widetilde{\mathbf{F}}(t) \tag{1}$$

In our first study case, which we will call Case I, the electronic stopping is activated at the beginning of the simulation, and it is still active when the e-ph coupling is activated at t_{eph}. The electronic stopping is applied only to atoms that move with velocity larger than a specified cut-off value v_c:

$$\gamma_i = \gamma_s + \gamma_p \quad \text{with} \quad \gamma_s = 0 \quad \text{for} \quad v_i \leq v_c, \tag{2}$$

where m_i is the mass of atom i with velocity v_i, and the value of v_c corresponds to energy double the cohesive energy of the target system [18]. An atom with velocity corresponding to twice the cohesive energy will travel distance equivalent to the range of the interatomic potential in the time needed for the neighboring atoms to respond to the impulse of the moving atom [10]. Other suggested values for this parameters can be found in [19–22].

In the second case, which we will refer to as Case II, the electronic stopping, similar to Case I, is activated at the beginning of the simulation and is applied to atoms with velocities larger than v_c, but it is turned-off at t_{eph}, when the e-ph coupling is turned-on:

$$\gamma_i = \gamma_s \quad \text{for} \quad t < t_{eph} \quad \text{and} \quad \gamma_i = \gamma_p \quad \text{for} \quad t \geq t_{eph}, \quad \text{with} \quad \gamma_s = 0 \quad \text{for} \quad v_i \leq v_c \tag{3}$$

We additionally investigate the effect of the e-ph activation time in the damage production from 50 keV Ni cascades in Ni and equiatomic NiFe, for two activation times, 0.2 ps and 1 ps, both for Case I and for Case II. For very short times at the beginning of the simulation, the lattice temperature is ill-defined. Additionally, the e-ph coupling activation should allow time for the atoms to thermalize and transfer energy to the electrons. Typically, the thermal equilibrium is reached within 0.1 ps – 0.5 ps [23, 24]. We have chosen the first activation time (0.2 ps) by looking at the thermalization (convergence of kinetic and potential energies) in the cascades where the electronic stopping only is activated. The second activation time (1 ps) was chosen to be near the peak of the displacements, and before the system relaxation starts (see supplementary materials Figure S1 for the temporal evolution of the displaced atoms in a representative 50 keV Ni ion cascade). We have simulated ten randomly selected velocity directions of the primary knock-on atoms in systems of about 3.6 million atoms. Scaling of the energy in a Gaussian distribution is used at the MD box boundaries, within a layer of 8 Å, to prevent energy returning to the MD box, imitating bulk samples. An EAM (embedded atom method) type potential fitted for Ni-Fe-Cr systems has been used [25]. Prior to irradiation, all systems were relaxed at 300 K in the isobaric-isothermal ensemble (NPT) with 1 fs timestep, using the Berendsen algorithm with 1 ps relaxation time of the barostat and the thermostat.

The irradiation temperature is 300 K, meaning that initially both the atomic and electronic systems have the same temperature. As described in [15], the friction coefficient for both systems is 0.6 ps^{-1}, and is calculated with the SRIM code [26]. The cut-off velocity corresponds to twice the cohesive energy of the system [18] and is equal to 54 Å ps^{-1}. The e-ph coupling parameters for Ni and NiFe are 10.85×10^{17} W m $^{-3}$ K^{-1} and 8.78×10^{17} W m $^{-3}$ K^{-1} [15], respectively. The specific heat capacity for both systems for a range of the electronic temperature is shown in Figure 1, and was obtained from coherent potential approximation (CPA) [27, 28] calculations, as described elsewhere [29]. For the electronic thermal conductivity we used κ_e = 88 W m^{-1} K^{-1} and 21 W m^{-1} K^{-1} [30], for Ni and NiFe, respectively.

In Figure 2 (a) and (b) we present the surviving damage at the end of the simulated time for Ni and NiFe, respectively, in terms of the number of defects identified

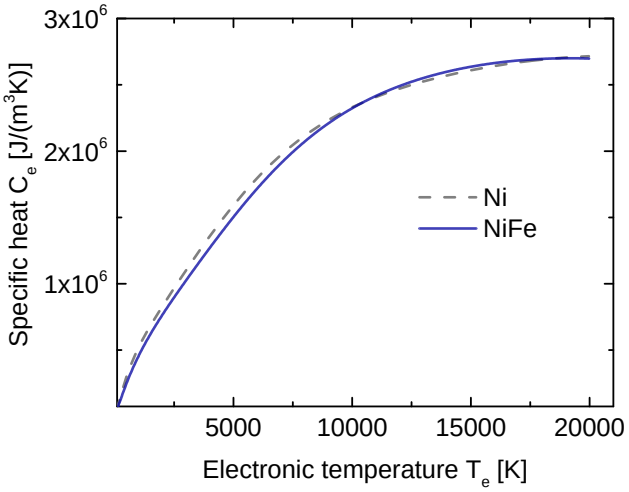

FIG. 1: Specific heat capacity for a range of the electronic temperature for Ni (grey dashed line) and equiatomic NiFe (blue solid line).

using the Wigner-Seitz method. For comparison, we have provided the average number of surviving Frenkel pairs for ten classic MD simulations from Ref. [15], where the electronic effects are ignored. Both in Ni and NiFe, Case I and Case II result in similar amount of surviving damage, for both activation times 0.2 ps and 1 ps. As shown in Figure 3, the number of atoms that have velocities equal or higher than the cut-off value in the cascade events in Ni and NiFe is very small, varying between 4 and 162 atoms. Such a small percentage of atoms on which the electronic stopping applies at 0.2 ps results in negligible difference in the surviving number of defects, which can be also attributed to the statistical difference of the irradiation events. At 1 ps, the highly energetic period of the cascade has finished, and there are no atoms with velocities higher than the cut-off. Therefore, the resulting difference between Case I and Case II shown in Fig. 2 (a) and (b) for e-ph coupling activation at 1 ps is due to statistical difference of the cascades.

Figure 2 (a) indicates that, in Ni, activation of the e-ph coupling at 1 ps results in a larger amount of damage compared to that for 0.2 ps activation time. While the cascade is quenched faster for 0.2 ps e-ph activation time, energy also can come back to the lattice sooner than in the case of 1 ps activation, where the electronic system has more time to dissipate energy away via the electronic grid before starting the return of energy to the atomic system. These two factors combine to result in a larger amount of damage for 1 ps activation time. For NiFe (Fig. 2 (b)), this difference is smaller than for Ni (Fig. 2 (a)), possibly due to the faster heat conduction that takes place in Ni. The larger value of the thermal conductivity of Ni means more rapid heat transfer. Fig. 4 (a) and (b) show the maximum electronic temperature per voxel in

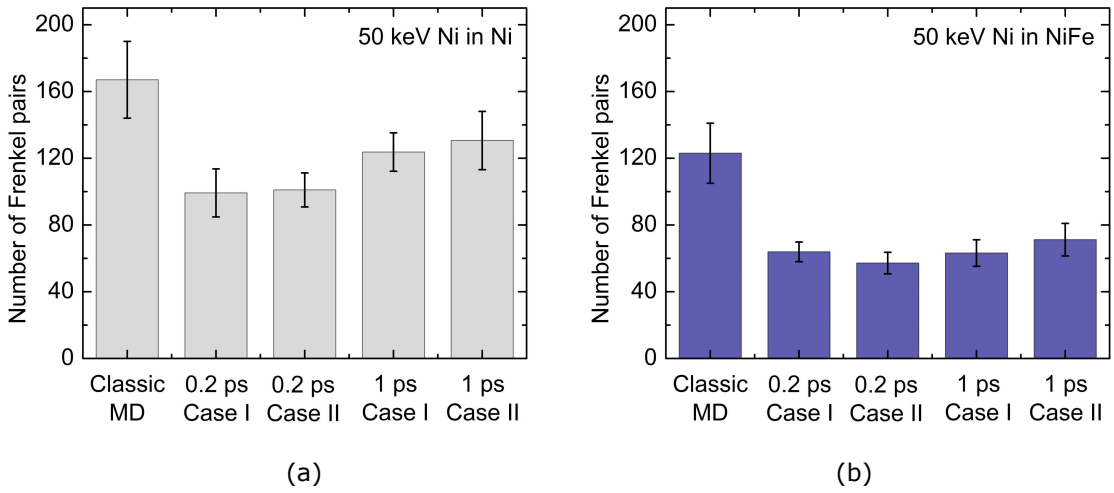

FIG. 2: Average surviving number of defects (Frenkel pairs) at the end of the simulation time for 50 keV Ni cascades in (a) Ni and (b) NiFe. The error bars represent the standard error over ten cascade events. Results for classical MD simulations from Ref. [15] is provided for comparison.

Ni and NiFe, where it is seen that the electronic temperature drops faster in Ni than in NiFe. Fig 4 (c) and (d) illustrate the corresponding maximum atomic temperature. Comparison of the maximum atomic temperature for the 1 ps e-ph activation time (Fig 4(e)) shows that for longer time (after the creation of the thermal spike within the first few ps), the atomic temperature of NiFe is higher, possibly enhancing the defect recombination.

Fig. 5 shows the electronic and atomic temporal evolution of the center cell of the MD box, for representative cascades in the two systems, for 0.2 ps and 1 ps e-ph coupling activation time. For the early activation of e-ph interactions, early energy exchange between the two subsystems is allowed, and the atomic temperature starts increasing at 0.2 ps. In the case of later activation, the energy transfer from the electrons to the atoms does not take place until 1 ps time. In these figures we see that the electronic temperature in Ni drops faster than in NiFe.

In Table I we have summarized the results of cluster analysis, where the second nearest-neighbor distance criterion for the identification of clusters was used. The fraction of isolated defects does not differ significantly in Case I and Case II, for both activation times of the e-ph coupling (0.2 ps and 1 ps), both in Ni and NiFe, but it is slightly lower for 1 ps activation time than for 0.2 ps. The total number of clusters consisting of more than three interstitials or vacancies does not change significantly between Case I and Case II, except for the 0.2 ps e-ph activation time in NiFe, where less interstitial and vacancy clusters are produced. In the case of e-ph coupling activation at 0.2 ps, the cascade is quenched at an early stage of its evolution. At 1 ps activation time, the energy exchange still happens within the thermal spike formation, but closer to the peak of the displacements (as seen in Figure S1). The earlier the e-ph coupling is activated, the earlier the cascade-induced shock wave is quenched, affecting at the same time the in-cascade cluster formation.

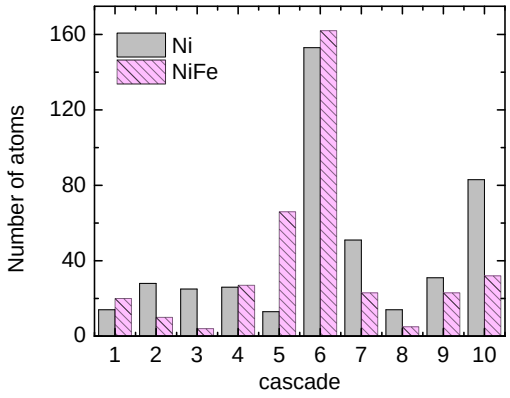

FIG. 3: Number of atoms with velocity higher than the cut-off value at 0.2 ps simulation time in 50 keV Ni ion cascades in Ni and NiFe. For 1 ps activation time, all atoms have velocities smaller than the specified cut-off.

Overall, for 50 keV Ni ion 2T-MD model cascade events, deactivation of the electronic stopping when the e-ph coupling is turned-on results in insignificant difference in the surviving damage, and has negligible effect in the defect clustering. Activation of the e-ph coupling at 1 ps compared to 0.2 ps results in slightly larger number of defects in Ni, and in NiFe the amount of produced damage is the same within error. While the activation time of the e-ph interaction can affect the amount of the produced damage, it should allow time for the thermal equilibrium of the lattice and the electrons to be reached, which typically takes place within 0.1 ps – 0.5 ps [23, 24].

	2T-MD			
	0.2 ps Case I	**0.2 ps** Case II	**1 ps** Case I	**1 ps** Case II
50 keV Ni	**Ni**			
Number of Frenkel Pairs	99 (13)	101 (10)	124 (12)	131 (7)
Fraction of isolated SIAs	0.18 (0.03)	0.16 (0.03)	0.12 (0.02)	0.09 (0.01)
Fraction of isolated vacancies	0.56 (0.05)	0.53 (0.05)	0.48 (0.05)	0.44 (0.05)
Number of SIA clusters (containing more than 3 SIAs)	56	61	52	65
Number of vacancy clusters (containing more than 3 vacancies)	27	26	36	41
50 keV Ni	**NiFe**			
Number of Frenkel Pairs	64 (5)	57 (6)	63 (8)	71 (10)
Fraction of isolated SIAs	0.40(0.03)	0.40 (0.06)	0.32 (0.04)	0.28 (0.04)
Fraction of isolated vacancies	0.52 (0.03)	0.52 (0.05)	0.48 (0.05)	0.48 (0.04)
Number of SIA clusters (containing more than 3 SIAs)	49	25	37	40
Number of vacancy clusters (containing more than 3 vacancies)	47	20	29	27

TABLE I: Surviving number of Frenkel pairs and cluster analysis for 50 keV Ni ion 2T-MD model cascades in Ni and equiatomic NiFe. The standard error of the mean calculated over ten events is provided in brackets. The cluster statistics are for clusters containing four or more self interstitial atoms (SIAs) or vacancies.

The effect of deactivation of the electronic stopping when the e-ph coupling is switched-on in the damage production should be further investigated in higher energy irradiation events, where higher electronic temperatures are expected, and therefore the electronic effects are more profound.

This work was supported by Energy Dissipation to Defect Evolution (EDDE), an Energy Frontier Research Center funded by the U.S. Department of Energy, Office of Science, Basic Energy Sciences. The simulation used resources of the National Energy Research Scientific Computing Center, supported by the Office of Science, US Department of Energy, under Contract No. DEAC02-05CH11231.

[1] T. Diaz de la Rubia and M.W. Guinan J. Nucl. Mater. 174 (1990) 151-157.
[2] 1.13-Radiation Damage Theory, in: R.J. Konings (Ed.), Comprehensive Nuclear Materials, Elsevier, Oxford, 2012, pp. 293-332.
[3] K. Nordlund and R.S. Averback, Phys. Rev. B 56 (1997) 2421.
[4] R. Devanathan, W.J. Weber, T. Diaz de la Rubia Nucl. Instr. Meth. B 141 (1998) 118-122.
[5] K. Trachenko, M. T. Dove, E. Artacho, I. T. Todorov, W. Smith, Phys. Rev. B 73 (2006) 174207.
[6] A. Chartier, J.-P. Crocombette, C. Meis c, W.J. Weber, L.R. Corrales Nucl. Instr. Meth. B 250 (2006) 1723.
[7] 1.11-primary radiation damage formation, in: R.J. Konings (Ed.), Comprehensive Nuclear Materials, Elsevier, Oxford, 2012, pp. 293-332.
[8] K. Trachenko, E. Zarkadoula, I.T. Todorov, M.T. Dove, D.J. Dunstan, K. Nordlund, Nucl. Instr. Meth. B 277 (2012) 613.
[9] E. Zarkadoula, S. L. Daraszewicz, D. M. Duffy, M. A. Seaton, I. T. Todorov, K. Nordlund, M. T. Dove and K Trachenko, J. Phys.: Condens. Mat. 25 (2013) 125402.
[10] D. M. Duffy and A. M. Rutherford, J. Phys.: Condens. Mat. 19 (2007) 016207.
[11] A. M. Rutherford and D. M. Duffy, J. Phys.: Condens. Mat. 19 (2007) 496201.
[12] E. Zarkadoula, S. L. Daraszewicz, D. M. Duffy, M. A. Seaton, I. T. Todorov, K. Nordlund, M. T. Dove and K Trachenko, J. Phys.: Condens. Matter 26 (2014) 085401.
[13] E. Zarkadoula, D. M. Duffy, K. Nordlund, M. A. Seaton, I. T. Todorov, W. J. Weber, and K Trachenko, J. Phys.: Condens. Matter 27 (2015) 135401.
[14] A. M. Stoneham, Nucl. Instrum. Methods B 48 (1989) 389.
[15] E. Zarkadoula, G. Samolyuk, H. Xue, H. Bei, W. J. Weber, Scripta Mater. 124 (2016) 6-10.
[16] E. Zarkadoula, G. Samolyuk, H. Xue, H. Bei, W. J. Weber, J. Alloys Compd. 700 (2017) 106-112.
[17] I. T. Todorov, B. Smith, M. T. Dove and K. Trachenko, J. Mater. Chem. 16 (2006)1911.
[18] E. Zhurkin and A. Kolesnikov, Nucl. Instr. Methods Phys. Res., Sect. B, 202 (2003) 269–277.
[19] M. Jakas and D. Harrison, Phys. Rev. B, **32** 2752–2760, (1985).
[20] K. Nordlund, L. Zhong, and R. Averback. Phys. Rev. B,

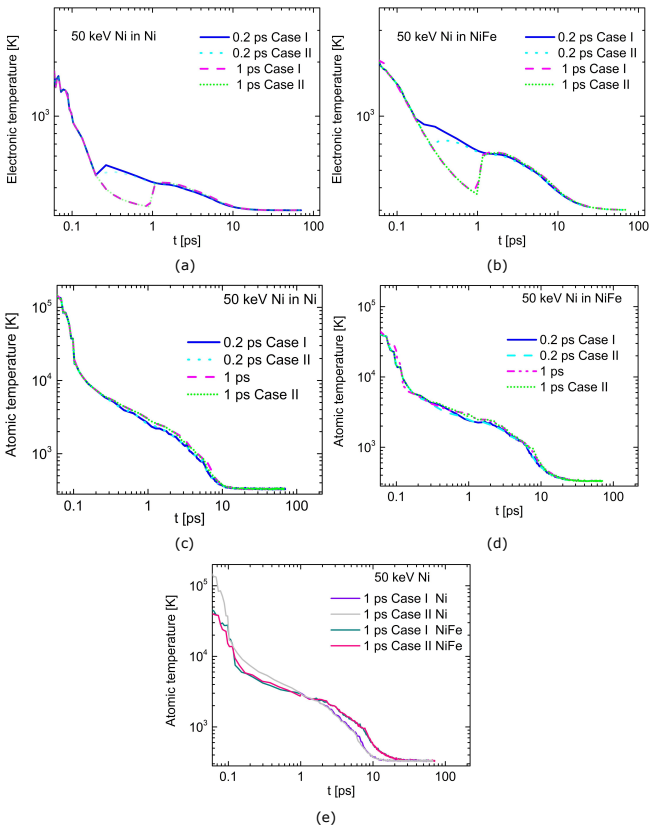

FIG. 4: Maximum electronic temperature for representative 50 keV Ni ion 2T-MD model cascades in (a) Ni and (b) NiFe. Corresponding maximum ionic temperature in (c) Ni and (d) NiFe. (e) Comparison between the maximum atomic temperature for 1 ps e-ph coupling activation time shown in (c) and (d).

57 965–968, (1998).

[21] J. le Page, D. R. Mason, C. P. Race, and W. M. C. Foulkes, New Journal of Physics, **11**, 1, 013004, (2009)

[22] C. Björkas, K. Nordlund, Nucl. Instrum. Methods Phys. Res., Sect. B, 267 **10**, 1830–1836, (2009)

[23] M. Toulemonde, W. Assman, C. Dufour, A. Meftah, F. Studer, and C. Trautmann, Mat. Fys. Medd. K. Dan. Vidensk. Selsk., 52 (2006) 263-292.

[24] M. Toulemonde, W. Assman, C. Dufour, A. Meftah, and C. Trautmann, Nucl. Instr. Methods Phys. Res., Sect. B, 277 (2012) 28-39.

[25] G. Bonny, N. Castin, D. Terentyev, Model. Simul. Mater. Sci. Eng. 21 (2013) 85004.

[26] http://www.srim.org/

[27] P. Soven. Phys. Rev. 156 (1967) 809.

[28] D. W. Taylor. Phys. Rev. 156 (1967) 1017.

[29] G. D. Samolyuk, L. K. Béland, G. M. Stocks, and R. E. Stoller, J. Phys.: Condens. Mat., 28 (2016) 175501.

[30] K. Jin, B. C. Sales, G. M. Stocks, G. D. Samolyuk, M. Daene, W. J. Weber, Y. Zhang and H. Bei, Sci. Rep. 6 (2016) 20159.

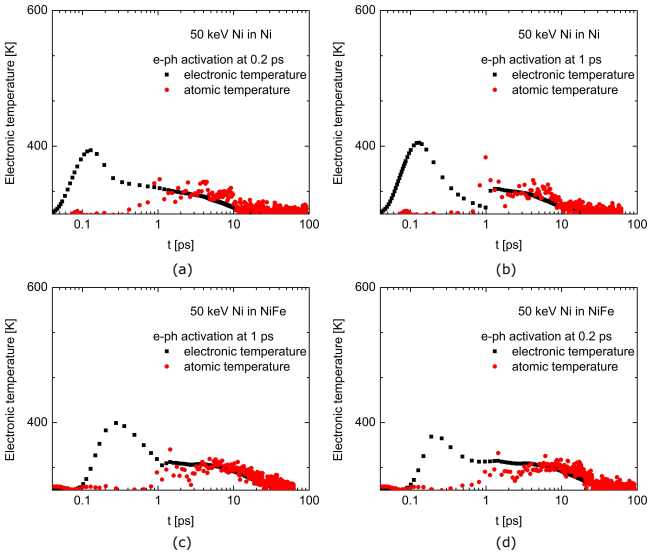

FIG. 5: Temporal evolution of the electronic and atomic temperature of the center cell of the MD box for representative cascades in Ni (a, b) and in NiFe (c,d) for both e-ph coupling activation times. The cascade is initiated near the corner of the MD box.